Proceedings of the National Conference on Computational Modeling of Fluid Dynamics Problems (CMFDP-2019)
NIT Warangal, India – Jan 18-20, 2019
Paper No. XXX (The number assigned when the papaer is accepted)

Effects of Couple-Stress in Peristaltic Transport of Blood Flow in Two Layered Model

K. Maruthi Prasad1[a] and N. Subadra 2[b*]
[a]Department of Mathematics, School of Technology, GITAM University, Hyderabad Campus, Hyderabad, Telangana, India-502329.
[b]Department of Mathematics, Geethanjali College of Engineering and Technology, Cheeryal (V), Keesara (M), R.R. Dist., Telangana, India-501301.

*Corresponding author Email: nemani.subhadra@gmail.com

Received: Date? Accepted: Date?

Abstract: Effects of couple-stress in peristaltic transport of blood flow in two layered model has been investigated by considering couple-stress fluid with nanoparticles in the core region and Newtonian fluid in the peripheral region under the assumption of long wavelength and low Reynolds number. The equations governing the flow are solved and closed form expressions for velocity in the peripheral region and in the core region, pressure drop, time averaged flux, frictional force, heat and mass transfer coefficients have been obtained. The effects of various parameters like couple-stress fluid parameters $\bar{\alpha}, \bar{\eta}$, viscosity ratio, mean radius of the central layer, local temperature Grashof number, local nano particles Grashof number, Brownian motion parameter and thermophoresis parameter on these flow variables have been studied. Streamline patterns and trapping phenomena have been studied and sketched through graphs at the end.

***Keywords*:** Peristalsis, Couple-stress Fluid, Nanoparticles, Peripheral Layer.

1. Introduction

Peristalsis is an important mechanism for fluid transport which is generated by the propagation of waves along the walls of a flexible tube containing fluid. Physiologically, it is an automatic and important process. The mechanism of peristaltic transport has been applied for industrial applications like transport of corrosive and noxious fluids, sanitary fluid transport and pumping of blood in heart lung machine. Several researchers have investigated the peristaltic motion of both Newtonian and non-Newtonian fluids in mechanical as well as physiological situations.

Stokes, [1] was the pioneer to develop couple-stress fluid as a special case of non-Newtonian fluid. A size dependent effect is introduced using couple stress which is not present in the classical viscous theories. Noted researchers like Srivastava, [2], Alemayehu & Radhakrishnamacharya, [3]) and Maiti & Misra, [4] studied couple-stress fluid problems.

Addition of nanoparticles to the base fluids with low thermal conductivity, enhances the thermal conductivity of the base fluids. Nanofluids have many biomedical and industrial applications. So many researchers are concentrated the study of nanofluids. (S. U.S. Choi, [5], Buongiorno, [6], Das et al., [7], Noreen, [8], Nadeem et al., [9], Prasad et al., [10]).

It is known that the nature of the fluid near the wall is different as compared to the core region of the tube in many physiological fluids. Hence, some investigators studied the effect of peripheral layer on peristaltic transport with particular reference to physiological systems. (Srivastava & Srivastava, [11], Rao &Usha, [12], Prasad &Radhakrishnamacharya, [13], Santhosh et al., [14]).

Keeping the above in view, a mathematical model of two immiscible fluids having couple-stress fluid with nanoparticles in the core region, Newtonian fluid in the peripheral layer has been

considered. Coupled equations of temperature profile and nanoparticle phenomena have been solved using homotopy perturbation method. The analytical solutions of velocity in peripheraland in core regions, pressure drop, frictional force, mechanical efficiency and effect of heat and mass transfers are obtained. The effects of different parameters on these flow variables are studied and represented graphically.

2. Mathematical Formulation

Consider the peristaltic transport in a tube, with an incompressible Newtonian fluid in the peripheral layer and couple-stress fluid with nanoparticles in the core region (Fig.1). Choosing the cylindrical polar coordinate system$(\bar{R}, \bar{\theta}, \bar{Z})$, the wall deformation due to the propagation of an infinite train of peristaltic waves is given by

$$\bar{R} = \bar{h}(\bar{Z}, \bar{t}) = a + b\, Sin\, \frac{2\pi}{\lambda}(\bar{Z} - c\bar{t}) \tag{1}$$

where, 'a' is the radius of the tube, b is the amplitude, λ is the wavelength and c is the speed of the wave.

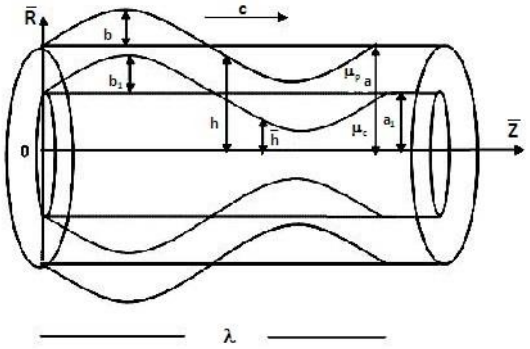

Fig. 1: Peristaltic transport of a couple-stress fluid with nanoparticles

The geometry of the interface between core region and peripheral layer is taken as Srivastava and Srivastava [11].

$$\bar{R} = \overline{h_1}(\bar{Z}, \bar{t}) = a_1 + b_1\, Sin\, \frac{2\pi}{\lambda}(\bar{Z} - c\bar{t}) \tag{2}$$

where, a_1 is the mean radius and b_1 is the amplitude of the central layer.

Using the transformations

$\bar{z} = \bar{Z} - c\bar{t}, \quad \bar{r} = \bar{R}, \quad \bar{\theta} = \bar{\theta}, \ \overline{w_1} = \overline{W_1} - c, \bar{w} = \bar{W} - c, \quad \bar{u} = \bar{U},$

from a stationary to moving frame of reference, the equations of motion in peripheral region and core region are given as follows:

Using the transformations

$\bar{z} = \bar{Z} - c\bar{t}, \quad \bar{r} = \bar{R}, \quad \bar{\theta} = \bar{\theta}, \ \overline{w_1} = \overline{W_1} - c, \bar{w} = \bar{W} - c, \quad \bar{u} = \bar{U},$

from a stationary to moving frame of reference, and applying non-dimensional quantities and the long wavelength and low Reynolds number approximations, the equations of motion in peripheral region and core region are given as follows:

$$\frac{\partial p}{\partial z} = \frac{1}{r}\frac{\partial}{\partial r}\left(\bar{\mu} r \frac{\partial}{\partial r}\right) w_1 \tag{3}$$

$$\frac{\partial P}{\partial r} = 0 \tag{4}$$

$$\frac{dp}{dz} + G_r\theta_t + B_r\sigma = \frac{1}{r}\frac{\partial}{\partial r}\left(r\frac{\partial}{\partial r}\left(1 - \frac{1}{\bar{\alpha}^2}\nabla^2\right) w_2\right) \tag{5}$$

$$0 = \frac{1}{r}\frac{\partial}{\partial r}\left(r\frac{\partial \theta_t}{\partial r}\right) + N_b\frac{\partial \sigma}{\partial r}\frac{\partial \theta_t}{\partial r} + N_t\left(\frac{\partial \theta_t}{\partial r}\right)^2 \tag{6}$$

$$0 = \frac{1}{r}\frac{\partial}{\partial r}\left(r\frac{\partial \sigma}{\partial r}\right) + \frac{N_t}{N_b}\left(\frac{1}{r}\frac{\partial}{\partial r}\left(r\frac{\partial \theta_t}{\partial r}\right)\right) \tag{7}$$

where, $\bar{\mu} = \frac{\mu_p}{\mu_c}$ is the viscosity ratio and $\bar{\alpha} = a\alpha = a\sqrt{\mu_c/\eta}$ is the couple-stress fluid parameter. Here w_1&w_2 are velocities in core and peripheral regions respectively. θ_t, σ, N_b, N_t, G_randB_r are temperature profile, nanoparticle phenomenon, Brownian motion parameter,

Thermophoresis parameter, local temperature Grashof number and local nanoparticle Grashof number.

The non-dimensional boundary conditions are

$$\frac{\partial w_2}{\partial r} = 0,\ \frac{\partial \theta_t}{\partial r} = 0,\ \frac{\partial \sigma}{\partial r} = 0 \ at\ r = 0, \tag{8}$$

$$w_1 = -1,\ \theta_t = 0,\ \sigma = 0 \ \ at\ r = h(z) = 1 + \varepsilon\ sin2\pi z, \tag{9}$$

$$\frac{\partial^2 w_2}{\partial r^2} - \frac{\bar{\eta}}{r}\frac{\partial w_2}{\partial r} = 0 \ \ at\ r = h_1(z) = \delta + \varepsilon_1\ sin2\pi z, \tag{10}$$

$$\frac{\partial^2 w_2}{\partial r^2} - \frac{\bar{\eta}}{r}\frac{\partial w_2}{\partial r}\ is\ finite\ \ at\ r = 0. \tag{11}$$

$$\bar{\mu}\frac{\partial w_1}{\partial r} = \frac{\partial}{\partial r}\left(w_2 - \frac{1}{\bar{\alpha}^2}\frac{1}{r}\left(\frac{\partial}{\partial r}\left(r\frac{\partial w_2}{\partial r}\right)\right)\right) + \frac{r}{2}(G_r\theta_t + B_r\sigma) \text{at} r = h_1(z) \tag{12}$$

$$w_1 = w_z\ at\ r = h_1(z) \tag{13}$$

where $\varepsilon(=\frac{b}{a})$ is the amplitude ratio, $\eta' = \frac{\bar{\eta}}{\eta}$ is a couple-stress fluid parameter, $\delta = \frac{a_1}{a}$ and $\varepsilon_1 = \frac{b_1}{a}$. Boundary conditions (10) and (11) indicate that the couple-stresses vanish at the tube wall and is finite at the tube axis respectively.

It is taken $h_1 = \delta h$ and $\varepsilon_1 = \delta\varepsilon$ by following the analysis of Shukla et al. [15].

3. Solution of the problem

Solving equation (3), subject to the boundary condition (9), the expression for w_1 is

$$w_1 = \frac{r^2 - h^2}{4\bar{\mu}}\frac{dp}{dz} + \frac{c_1}{\bar{\mu}}\ log\left(\frac{r}{h}\right) - 1 \tag{14}$$

The coupled equations of $\theta_t,\ \sigma$ i.e. Eqs. (5) & (6) are solved using Homotopy perturbation Method (HPM) with the initial guess $\theta_{10}(r,z) = \left(\frac{r^2-h^2}{4}\right),\ \ \sigma_{10}(r,z) = -\left(\frac{r^2-h^2}{4}\right)$, then the solution for $\theta_t,\ \sigma$ is given as

$$\theta_t(r,z) = \left(\frac{r^4 - h^4}{64}\right)(N_b - N_t) \tag{15}$$

$$\sigma(r,z) = -\left(\frac{r^2-h^2}{4}\right)\frac{N_t}{N_b} \tag{16}$$

Substituting Eqs. (15) & (16) in Eq. (5) and solving this and Eq. (14) by applying boundary conditions (8)-(13), the expression for velocities in the peripheral region and core regions are given as

$$w_1 = \frac{r^2 - h^2}{4\bar{\mu}}\frac{dp}{dz} + log\left(\frac{r}{h}\right)(C_1 + D) - 1 \tag{17}$$

$$w_2 = -1 + B[I_o(\bar{\alpha}r) - I_o(\bar{\alpha}h_1)] + \frac{C_1}{\bar{\alpha}}\ log\left(\frac{h_1}{h}\right) + \frac{dp}{dz}\left(\frac{r^2}{4} + G\right) + G_r(N_b - N_t)\left[\frac{r^2}{4\bar{\alpha}^4} - \frac{r^2{h_1}^4}{256} + \frac{r^4}{64\bar{\alpha}^2} + \frac{r^6}{2304} + E\right] + B_r\left(\frac{N_t}{N_b}\right)\left[-\frac{r^2}{4\bar{\alpha}^2} + \frac{r^2{h_1}^2}{16} - \frac{r^4}{64} + F\right] \tag{18}$$

where, $A = \bar{\alpha}\left[\bar{\alpha}I_o(\bar{\alpha}h_1) - \frac{1}{h_1}(1+\bar{\eta})I_1(\bar{\alpha}h_1)\right]$

$$B = -\frac{G_r}{A}(N_b - N_t)\left[\frac{1}{2\bar{\alpha}^4}(1-\bar{\eta}) + \frac{{h_1}^4}{192}(1+\bar{\eta}) + \frac{3{h_1}^2}{64}(1-3\bar{\eta})\right] - \frac{B_r}{A}\left(\frac{N_t}{N_b}\right)\left[\frac{1}{2\bar{\alpha}^2}(\bar{\eta}-1) - \frac{{h_1}^2}{16}(1+\bar{\eta})\right]$$

$$C_1 = \frac{B}{\bar{\mu}}\left[\frac{1}{\bar{\alpha}}(1 + h_1\bar{\alpha}^2)I_1(\bar{\alpha}h_1) - h_1 I_o(\bar{\alpha}h_1)\right],\ D = \frac{1}{\bar{\mu}}\left[-G_r(N_b - N_t)\frac{{h_1}^6}{192} + B_r\left(\frac{N_t}{N_b}\right)\frac{{h_1}^4}{16}\right]$$

$$E = -\frac{{h_1}^2}{4\bar{\alpha}^4} - \frac{{h_1}^4}{64\bar{\alpha}^2} + \frac{{h_1}^6}{288} - \frac{{h_1}^6}{\bar{\mu}}log\left(\frac{h_1}{h}\right),\quad F = \frac{{h_1}^2}{4\bar{\alpha}^2} - \frac{3{h_1}^4}{64} + \frac{{h_1}^4}{\bar{\mu}}log\left(\frac{h_1}{h},\right) G = -\frac{h^2}{4} + \frac{{h_1}^2}{4\bar{\mu}} - \frac{h^2}{4\bar{\mu}}$$

where, I_o and I_1 are modified Bessel functions of order zero and one respectively.

The dimension less flux $q$in the moving frame is given as

$$q = \int_0^{h_1} 2rw_2 dr + \int_{h_1}^{h} 2rw_1 dr \tag{19}$$

Substituting w_1 and w_2 from Eqs. (17) and (18) in Eq. (19), the expression for $\frac{dp}{dz}$ is

$$\frac{dp}{dz} = \frac{q}{S} - \frac{2B}{S}\left[h_1 I_1(\bar{\alpha}h_1) - \frac{{h_1}^2}{2} I_o(\bar{\alpha}h_1)\right] - \frac{C_1}{\bar{\alpha}}\frac{h_1}{S} log\left(\frac{h_1}{h}\right) + \frac{h^2}{S}$$
$$- \frac{2(C_1 + D)}{S}\left[-\frac{h^2}{2}\log h - \frac{{h_1}^2}{2}\log h_1 + {h_1}^2 \log h - \frac{1}{4}\left(h^2 - {h_1}^2\right)\right]$$
$$- \frac{G_r(N_b - N_t)}{S}\left[\frac{{h_1}^2}{8\bar{\alpha}^4} + \frac{{h_1}^6}{192} - \frac{17{h_1}^8}{9216} + {h_1}^2 E\right] - \frac{B_r}{S}\left(\frac{N_t}{N_b}\right)\left[-\frac{{h_1}^4}{8\bar{\alpha}^2} + \frac{5{h_1}^6}{192} + {h_1}^2 F\right] \quad (20)$$

where, $S = \frac{{h_1}^2 h^2}{4\bar{\mu}} - \frac{{h_1}^4}{4\bar{\mu}} - \frac{h^2}{4\bar{\mu}} + \frac{{h_1}^4}{8} + {h_1}^2 G$

The pressure drop over a wavelength ΔP_λ is defined as

$$\Delta P_\lambda = -\int_0^1 \frac{dP}{dz} dz \quad (21)$$

Substituting the expression $\frac{dp}{dz}$ from Eq. (20) into Eq. (21), the pressure drop is

$$\Delta P_\lambda = qL_1 + L_2 \quad (22)$$

where, $L_1 = \int_0^1 \frac{-1}{S}\, dz$

$$L_2 = -\int_0^1 \frac{2B}{S}\left[h_1 I_1(\bar{\alpha}h_1) - \frac{{h_1}^2}{2} I_o(\bar{\alpha}h_1)\right] dz - \int_0^1 \frac{C_1}{\bar{\alpha}}\frac{h_1}{S} log\left(\frac{h_1}{h}\right) dz + \int_0^1 \frac{h^2}{S} dz$$
$$- \int_0^1 \frac{2(C_1 + D)}{S}\left[-\frac{h^2}{2}\log h - \frac{{h_1}^2}{2}\log h_1 + {h_1}^2 \log h - \frac{1}{4}\left(h^2 - {h_1}^2\right)\right] dz$$
$$- \int_0^1 \frac{G_r(N_b - N_t)}{S}\left[\frac{{h_1}^2}{8\bar{\alpha}^4} + \frac{{h_1}^6}{192} - \frac{17{h_1}^8}{9216} + {h_1}^2 E\right] dz - \int_0^1 \frac{B_r}{S}\left(\frac{N_t}{N_b}\right)\left[-\frac{{h_1}^4}{8\bar{\alpha}^2} + \frac{5{h_1}^6}{192} + {h_1}^2 F\right] dz$$

Following the analysis of Shapiro et al.(1969), the time averaged flux over a period in the laboratory frame $\bar{Q}$ is given as

$$\bar{Q} = 1 + \frac{\epsilon^2}{2} + q \quad (23)$$

The dimensionless frictional force $\bar{F}$ at the wall is

$$\bar{F} = \int_0^1 h^2 \left(-\frac{dP}{dz}\right) dz \quad (24)$$

The Heat and Mass transfer coefficient at the wall are given as

$$Z_\theta(r, z) = \left(\frac{\partial h}{\partial z}\right)\left(\frac{\partial \theta_t}{\partial r}\right) \quad (25)$$

$$Z_\sigma(r, z) = \left(\frac{\partial h}{\partial z}\right)\left(\frac{\partial \sigma}{\partial r}\right) \quad (26)$$

4. Results and Discussions

Analytical expressions for velocity in the peripheral region and core region, pressure drop, time averaged flux, frictional force, heat and mass transfer coefficients have been calculated. Various graphs are depicted by using Mathematica 9.0 software.

Effects of various parameters on pressure drop characteristics are shown in Figs. 2.1-2.8. Pressure drop (Δp_λ) increases with the increases of couple-stress fluid parameter($\bar{\alpha}$), viscosity ratio($\bar{\mu}$), mean radius of the central layer(δ), local temperature Grashof number(G_r), local nanoparticle Grashof number(B_r) and thermophoresis parameter (N_t), whereas pressure drop(Δp_λ) decreases with the increase of couple-stress fluid parameter ($\bar{\eta}$) and Brownian motion parameter (N_b).

It is noticed from Figs. (3.1)–(3.8) that, Frictional force($\bar{F}$) increases with the increases of $\bar{\alpha},\ \bar{\mu},\ \delta, G_r, B_r, N_t$, whereas it decreases with the increase of $\bar{\eta}$ and N_b.

It is observed from Figs. (4.1)-(4.3) that, Heat transfer coefficient (Z_θ)value increases with the increase of $N_b$and N_t and then decreases after attaining a constant value. However it shows an opposite behaviour with respect to amplitude ratio (ε).

It is also observed from Figs. (5.1)-(5.3) that, Mass transfer coefficient (Z_σ)value increases with the increase of N_b, ε and then decreases after attaining a constant value $r = 0$. However, it shows an opposite behaviour with respect to N_t.

It is noticed from Figs. (6.1)-(6.9) that, the size of the trapped bolus increases with the increase of $\bar{\alpha}, \bar{\eta}$, $\bar{\mu}$, δ, G_r, N_b, ε ,and decreases with the increase of B_r and N_t.

5. Graphs

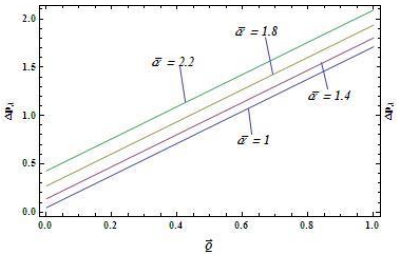

Fig. 2.1: Effect of $\bar{Q}$ and $\bar{\alpha}$ on (Δp_λ)
$(\varepsilon = 0.05, \bar{\eta} = 0.8, G_r = 0.5, B_r = 0.3, N_b = 0.3, N_t = 0.8, \delta = 0.8, \bar{\mu} = 0.5)$

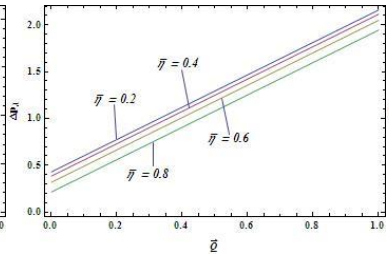

Fig. 2.2: Effect of $\bar{Q}$ and $\bar{\eta}$ on (Δp_λ)
$(\varepsilon = 0.1, \bar{\alpha} = 1.8, G_r = 0.5, B_r = 0.3, N_b = 0.3, N_t = 0.8, \delta = 0.8, \bar{\mu} = 0.5)$

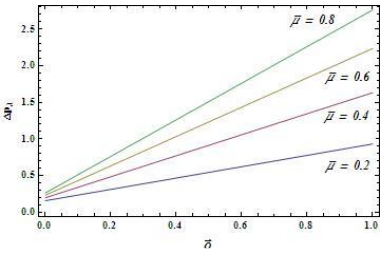

Fig. 2.3: Effect of $\bar{Q}$ and $\bar{\mu}$ on (Δp_λ)
$(\varepsilon = 0.1, \bar{\eta} = 0.8, G_r = 0.5, B_r = 0.3, N_b = 0.3, N_t = 0.8, \delta = 0.8, \bar{\alpha} = 1.8)$

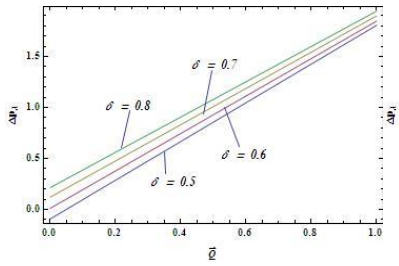

Fig. 2.4: Effect of $\bar{Q}$ and δ on (Δp_λ)
$(\varepsilon = 0.1, \bar{\eta} = 0.8, G_r = 0.5, B_r = 0.3, N_b = 0.3, N_t = 0.8, \bar{\mu} = 0.5, \bar{\alpha} = 1.8)$

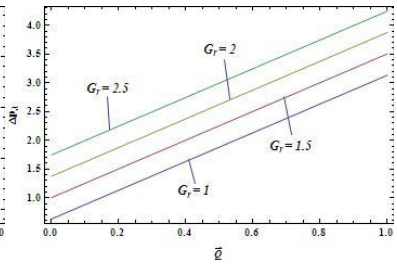

Fig. 2.5: Effect of $\bar{Q}$ and G_r on (Δp_λ)
$(\varepsilon = 0.1, \bar{\eta} = 0.8, \delta = 0.8, B_r = 0.3, N_b = 0.3, N_t = 0.8, \bar{\mu} = 0.8, \bar{\alpha} = 1.8)$

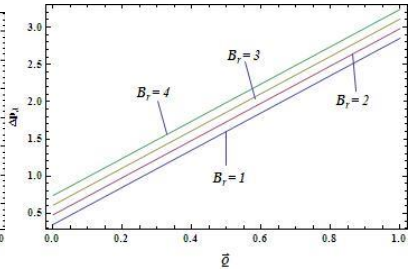

Fig. 2.6: Effect of $\bar{Q}$ and B_r on (Δp_λ)
$(\varepsilon = 0.1, \bar{\eta} = 0.8, \delta = 0.8, G_r = 0.5, N_b = 0.3, N_t = 0.8, \bar{\mu} = 0.8, \bar{\alpha} = 1.8)$

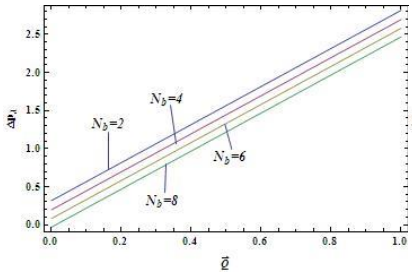

Fig. 2.7: Effect of $\bar{Q}$ and N_b on (Δp_λ)
$(\varepsilon = 0.1, \bar{\eta} = 0.8, \delta = 0.8, G_r = 0.5, B_r = 0.3, N_t = 0.8, \bar{\mu} = 0.8, \bar{\alpha} = 2.2)$

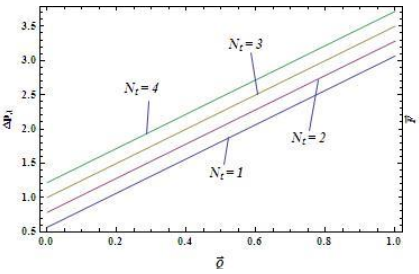

Fig. 2.8: Effect of $\bar{Q}$ and N_t on (Δp_λ)
$(\varepsilon = 0.1, \bar{\eta} = 0.8, \delta = 0.8, G_r = 0.5, B_r = 0.3, N_b = 0.3, \bar{\mu} = 0.8, \bar{\alpha} = 2.2)$

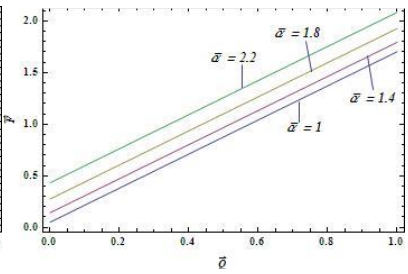

Fig. 3.1: Effect of $\bar{Q}$ and $\bar{\alpha}$ on$\bar{F}$
$(\varepsilon = 0.05, \bar{\eta} = 0.8, G_r = 0.5, B_r = 0.3, N_b = 0.3, N_t = 0.8, \delta = 0.8, \bar{\mu} = 0.5)$

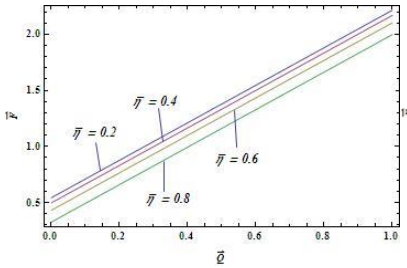

Fig. 3.2: Effect of $\bar{Q}$ and $\bar{\eta}$ on$\bar{F}$
$(\varepsilon = 0.1, \bar{\alpha} = 1.8, G_r = 0.5, B_r = 0.3, N_b = 0.3, N_t = 0.8, \delta = 0.8, \bar{\mu} = 0.5)$

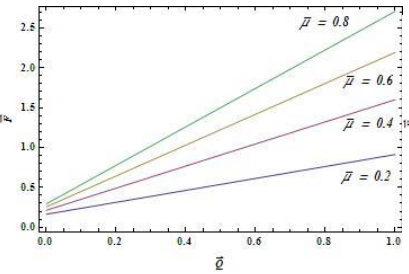

Fig. 3.3: Effect of $\bar{Q}$ and $\bar{\mu}$ on$\bar{F}$
$(\varepsilon = 0.1, \bar{\eta} = 0.8, G_r = 0.5, B_r = 0.3, N_b = 0.3, N_t = 0.8, \delta = 0.8, \bar{\alpha} = 1.8)$

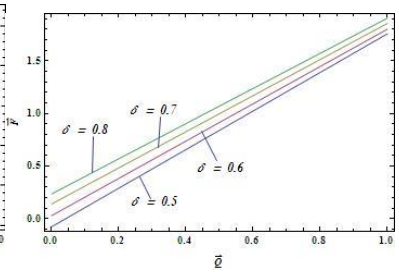

Fig. 3.4: Effect of $\bar{Q}$ and δ on$\bar{F}$
$(\varepsilon = 0.1, \bar{\eta} = 0.8, G_r = 0.5, B_r = 0.3, N_b = 0.3, N_t = 0.8, \bar{\mu} = 0.5, \bar{\alpha} = 1.8)$

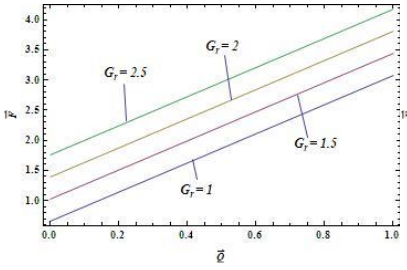

Fig. 3.5: Effect of $\overline{Q}$ and G_r on$\overline{F}$
$(\varepsilon = 0.1, \bar{\eta} = 0.8, \delta = 0.8, B_r = 0.3,$
$N_b = 0.3, N_t = 0.8, \bar{\mu} = 0.8, \bar{\alpha} = 1.8)$

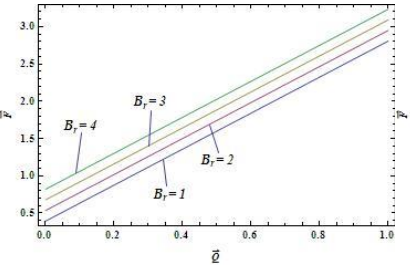

Fig. 3.6: Effect of $\overline{Q}$ and B_r on$\overline{F}$
$(\varepsilon = 0.1, \bar{\eta} = 0.8, \delta = 0.8, G_r = 0.5,$
$N_b = 0.3, N_t = 0.8, \bar{\mu} = 0.8, \bar{\alpha} = 1.8,$

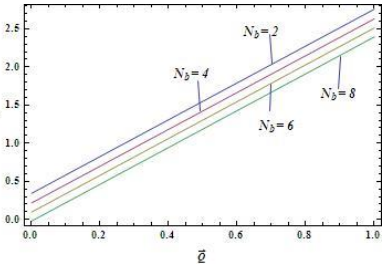

Fig. 3.7: Effect of $\overline{Q}$ and N_b on$\overline{F}$
$(\varepsilon = 0.1, \bar{\eta} = 0.8, \delta = 0.8, G_r = 0.5,$
$B_r = 0.3, N_t = 0.8, \bar{\mu} = 0.8, \bar{\alpha} = 2.2)$

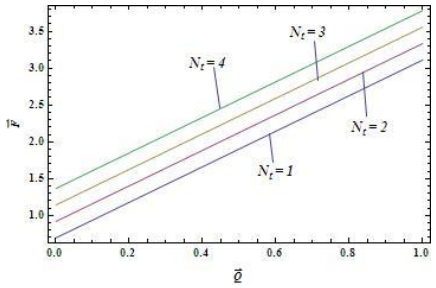

Fig. 3.8: Effect of $\overline{Q}$ and N_t on$\overline{F}$
$(\varepsilon = 0.1, \bar{\eta} = 0.8, \delta = 0.8, G_r = 0.5,$
$B_r = 0.3, N_b = 0.8, \bar{\mu} = 0.8, \bar{\alpha} = 2.2)$

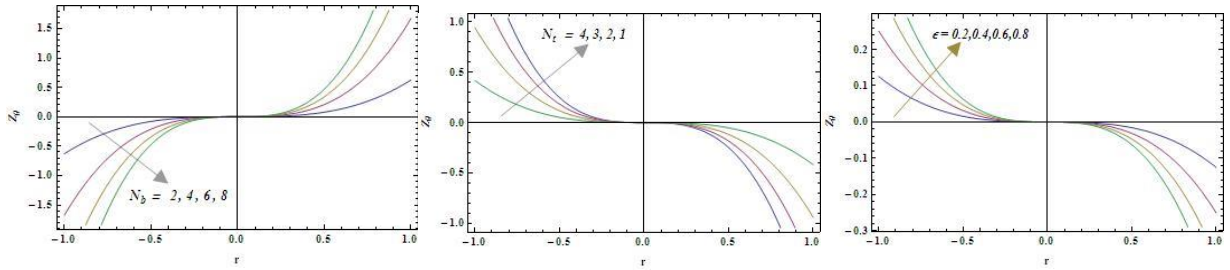

Fig. 4.1-4.3: Variation in heat transfer coefficient with N_b, N_t& ε

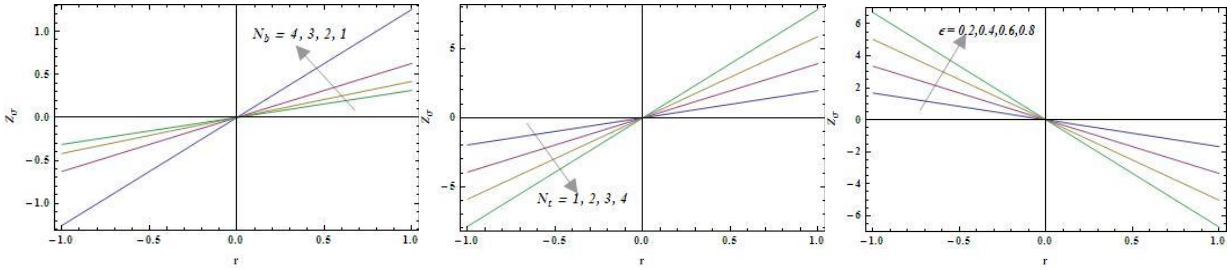

Fig. 5.1-5.3: Variation in Mass transfer coefficient with N_b, N_t& ε

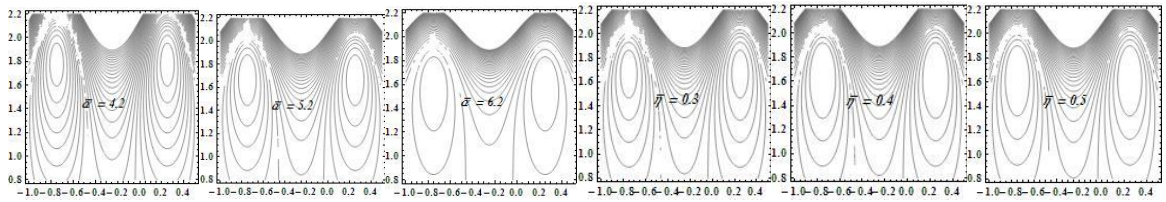

Fig. 6.1-6.2: streamline patterns for different values of $\bar{\alpha}$, $\bar{\eta}$

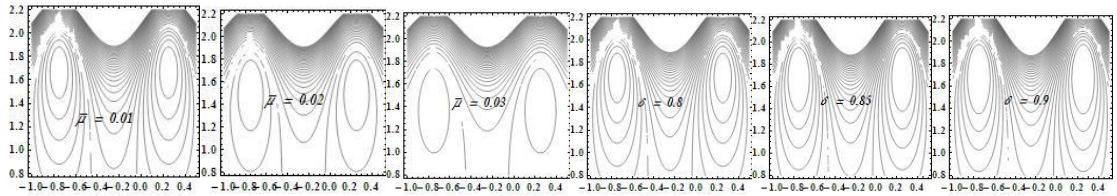

Fig. 6.3-6.4: streamline patterns for different values of $\bar{\mu}$, δ

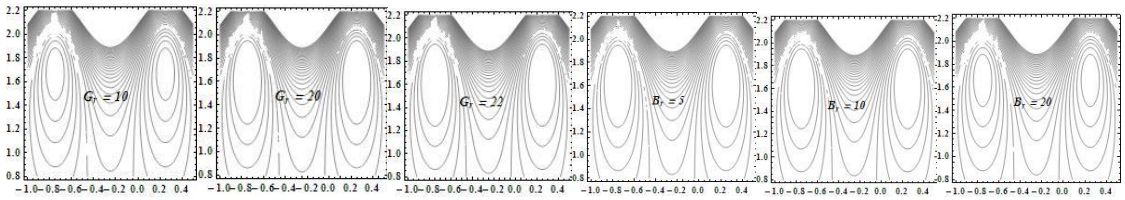

Fig. 6.5-6.6: streamline patterns for different values of G_r, B_r

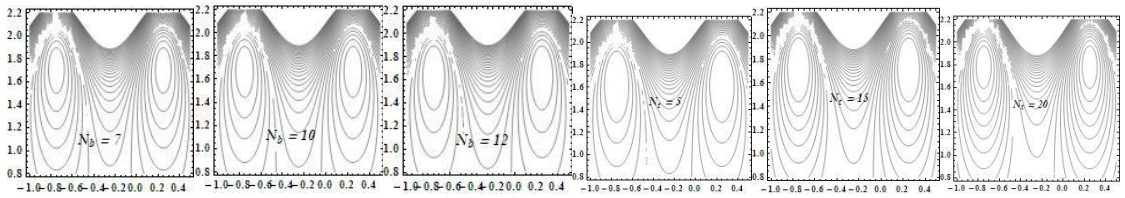

Fig. 6.7-6.8: streamline patterns for different values of N_b, N_t

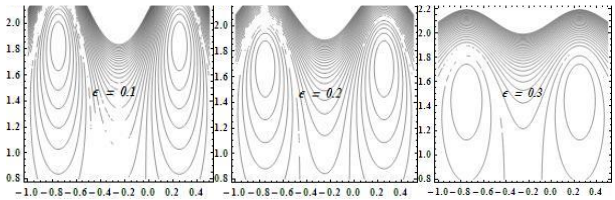

Fig. 6.9: streamline patterns for different values of ε

6. Conclusions

Effects of couple-stress in peristaltic transport of blood flow in two layered model has been investigated by considering couple-stress fluid with nanoparticles in the core region and Newtonian fluid in the peripheral region under the assumption of long wavelength and low Reynolds number.

The main points of the analysis are as follows:

a. Pressure drop increases with couple-stress fluid parameter $\bar{\alpha}$, viscosity ratio, mean radius of the central layer, local temperature Grashof number, local nanoparticle Grashof number and with thermophoresis parameter and decreases with the increase of couple-stress fluid parameter $\bar{\eta}$ and Brownian motion parameter.

b. Frictional force increases with couple-stress fluid parameter$\bar{\alpha}$, viscosity ratio, mean radius of the central layer, local temperature Grashof number, local nanoparticle Grashof number and with thermophoresis parameter and decreases with the increase of couple-stress fluid parameter $\bar{\eta}$and Brownian motion parameter.

c. The heat transfer coefficient value increases initially with the increase of Brownian motion parameter and thermophoresis parameter and then decreases after attaining a constant value. However heat transfer coefficient value shows an opposite behaviour with respect to amplitude ratio.

d. Mass transfer coefficient value increases initially with the increase of Brownian motion parameter, amplitude ratio and then decreases after attaining a constant value $r = 0$. However, mass transfer coefficientshows an opposite behaviour with respect to thermophoresis parameter.

e. The size of the trapped bolus increases with the increase of couple-stress fluid parameters$\bar{\alpha}, \bar{\eta}$, viscosity ratio, mean radius of the central layer, local temperature Grashof number, Brownian motion parameter and amplitude ratio.

f. The size of the trapped bolus decreases with the increase of local nanoparticle Grashof number and thermophoresis parameter.

References

[1] Stokes, V. K. (1966). Couple stresses in fluids. Physics of Fluids (1958-1988), 9(9), 1709–1715.

[2] Srivastava, L. M. (1986). Peristaltic transport of a couple-stress fluid. RheologicaActa, 25(6), 638–641. http://doi.org/10.1007/BF01358172

[3] Alemayehu, H., &Radhakrishnamacharya, G. (2010). Dispersion of a solute in peristaltic motion of a couple stress fluid through a porous medium with slip condition. International Journal of Chemical and Biological Engineering, 3(4), 205–210.

[4] Maiti, S., &Misra, J. (2012). Peristaltic transport of a couple stress fluid: some applications to hemodynamics. Journal of Mechanics in Medicine and Biology, 12(03), 1250048.

[5] S. U.S. Choi, J. A. E. (1995). Enhancing thermal conductivity of fluids with nanoparticles. ASME FED. Proceedings of the ASME International Mechanical Engineering Congress and Exposition,66.

[6] Buongiorno, J. (2005). Convective Transport in Nanofluids. Journal of Heat Transfer, 128(3), 240–250. http://doi.org/10.1115/1.2150834

[7] Das, S. K., Putra, N., & Roetzel, W. (2003). Pool boiling of nano-fluids on horizontal narrow tubes. International Journal of Multiphase Flow, 29(8), 1237–1247. http://doi.org/10.1016/S0301-9322(03)00105-8

[8] Noreen, S. (2013). Mixed Convection Peristaltic Flow of Third Order Nanofluid with an Induced Magnetic Field. PLoS ONE, 8(11), e78770. http://doi.org/10.1371/journal.pone.0078770

[9] Nadeem, S., Riaz, A., Ellahi, R., & Akbar, N. S. (2014). Mathematical model for the peristaltic flow of nanofluid through eccentric tubes comprising porous medium. Applied Nanoscience, 4(6), 733–743.

[10] Prasad, K. M., Subadra, N., &Srinivas, M. (2015). Peristaltic Transport of a Nanofluid in an Inclined Tube. American Journal of Computational and Applied Mathematics, 5(4), 117–128

[11] Srivastava, L. M., &Srivastava, V. P. (1982). Peristaltic transport of a two-layered model of physiological fluid. Journal of Biomechanics, 15(4), 257–265. http://doi.org/10.1016/0021-9290(82)90172-5

[12] Rao, A. R., &Usha, S. (1995). Peristaltic transport of two immiscible viscous fluids in a circular tube. Journal of Fluid Mechanics, 298, 271–285. http://doi.org/10.1017/S0022112095003302

[13] Prasad, K., &Radhakrishnamacharya, G. (2009). Effect of peripheral layer on peristaltic transport of a micropolar fluid.

[14] Santhosh, N., Radhakrishnamacharya, G., &Chamkha, A. J. (2015). Flow of A Jeffrey Fluid Through A Porous Medium in Narrow Tubes. Journal of Porous Media, 18(1), 71–78.

[15] Shukla, J. B., Parihar, R. S., Rao, B. R. P., & Gupta, S. P. (1980). Effects of peripheral-layer viscosity on peristaltic transport of a bio-fluid. Journal of Fluid Mechanics, 97(02), 225–237. http://doi.org/10.1017/S0022112080002534